Characterizing Spatial Parameters of Forest Canopies Using Fisheye Photography: Applications in Photo Ecometrics

John J. Battles

Department of Environmental Science, Policy, and Management
151 Hilgard Hall, University of California, Berkeley, CA 94720-3110, USA

Abstract
Five case studies are presented that demonstrate how metrics inferred from canopy photography can inform and validate the results from digital aerial photography and other remote sensing platforms. The forests measured include evergreen and deciduous canopies composed of both needle-leaved and broad-leaved tree species. Gap fractions of these forest canopies ranged from 3% to 22%. Significant fine-scale spatial autocorrelation of canopy structure was detected in two subalpine forests. In a conifer-hardwood forest, the canopy opening associated with the stream course still influenced understory light availability 45 m from the stream bank. In contrast, there was no correspondence between distance from the stream and canopy architecture in two *Tsuga*-dominated ravines. Forest stands classified as the same vegetation type and considered replicated sites in field experiments can have significant differences in some canopy metrics. The results from these ecological studies have direct relevance to the design of monitoring regimes based on remote sensing.

I. INTRODUCTION

Research in geographic information science crosses many traditional academic disciplines. Common challenges include the need to address spatially-explicit questions and to aggregate results through multiple scales of inquiry. Often this challenge involves measuring, monitoring, or modeling phenomena over large landscapes where adequate field sampling is economically impractical. Thus the practical solution demands the use of remote sensing technologies (Adams [1], Gong *et al.* [10]).

Applications of remote sensing in terrestrial ecology are sometimes viewed with skepticism by field ecologists. It is difficult to link information recorded from the ground, air, and space (Howard *et al.* [12]). Sometimes there is a mismatch between a parameter that can be remotely sensed and its ground-based equivalent. Other times an acceptable standard of accuracy for a regional monitoring program based on remotely sensed data seems woefully inadequate to an ecologist trying to answer a process-level question. One response to this skepticism is to generate a product, for example a global vegetation map, based completely on a remote sensing scheme (Nemani and Running [17]). While such an approach would allow rapid, efficient mapping and would ease the implementation of ecosystem models, such a map generally would be ignored by both vegetation scientists and resource managers (Adams [1]). A better solution is to develop new techniques with sufficient resolution and accuracy to meet the needs of both global ecology and community ecology.

Ecometrics is the science of deriving meaningful ecological parameters using remote sensing technologies (Gong *et al.* [10]). The subfield of photo ecometrics seems especially appropriate to applications in forested landscapes. Gong *et al.* [10] are conducting pioneering research in the use of high-resolution digital aerial photographs to measure important forest characteristics such as crown cover and canopy height. Ground-based fisheye photography is a complementary component of photo ecometrics for forest inventory. The goal of this paper is to demonstrate how the metrics inferred from canopy photography can inform and validate the results from digital aerial photography and other remote sensing platforms.

Rich [21] provides a thorough and detailed explanation of the methodology for characterizing plant canopies with fisheye photographs. In brief, fisheye (hemispherical) photographs are taken under the canopy looking up with an extreme wide-angle lens that provides an 180°viewing angle of the canopy. The geometric distributions of openings are precisely measured from the photograph and a suite of ecological variables can be calculated including canopy cover, leaf area index, and light penetration through the canopy. Because many photographs can be taken and processed with a reasonable effort, collecting a large

1082-4006/99/0501-30$3.00

sample to detect spatial trends is possible. Applications of this technique have ranged from an assessment of fine-scale microenvironments to landscape-level descriptions of canopy architecture.

This paper is organized around five case studies selected to demonstrate how the results from canopy photography can provide useful insights into the spatial structure and variability of forest canopies. The examples extend from a very fine-scale study (0.5 ha) to a landscape-level study encompassing a distinctly delimited forested site (47 km^2). The kinds of forest canopies measured include needle-leaved, evergreen forests; a broad-leaved, deciduous forest; a broad-leaved, evergreen forest; and a mixed canopy containing both broad-leaved deciduous trees and needle-leaved evergreen trees. The specific objective is to use these examples to illustrate applications of fisheye canopy photography to photo ecometrics under a range of forest conditions.

II. METHODS

Fisheye Canopy Photography

At each sample point, a fisheye photograph (Canon 7.5 mm lens or Nikkor 8mm lens) was taken of the canopy. Photographs were shot at approximately 1.2 m above the ground. Understory vegetation taller than 1.2 m and within an approximate 1-m radius of the sample point was pinned back to get an unobstructed view of the canopy. Pictures were taken near dawn and dusk to approximate uniform skylight conditions. The camera was leveled and oriented so that true north could be identified in the photograph. By trial and error, exposure settings were adjusted at each site to maximize the contrast between canopy elements and the sky. Photographs were taken using fine-grained black and white film.

The photographs were converted to digital images. For each picture, a threshold grey level was chosen that produced a digitized image that best approximated the actual photograph. Digitized images were cropped and converted to binary files with a final resolution of 512 by 512 pixels. Rich [20] discusses in detail protocols for photo acquisition and conversion to an electronic image.

Software provided by Canham [6] was used to compute the gap fraction, gap light index (GLI), and percent transmission of direct beam and diffuse radiation. Gap fraction refers to the fraction of sky unobstructed by canopy. GLI specifies the percentage of incident photosynthetically active radiation reaching a point in the understory during the growing season. The GLI ranges from 0 for a completely closed canopy to 100 for a completely open site. A necessary parameter for computing GLI is the global atmospheric transmission coefficient (K_T). K_T is the ratio of incident global radiation to total extraterrestrial radiation. I estimated the growing season K_T from daily solar flux data (when available) using the methodology described by Stoffel [27] or used published regional averages of K_T (Knapp *et al.* [13]) in the absence of site-specific data. To estimate the contribution of direct beam radiation to the total understory light budget, I used K_T to estimate the contribution of direct beam radiation to the incident global radiation (Spitters *et al.* [26]) and multiplied it by the fraction of incident light actually transmitted through the canopy (from the GLI routine). Note that the GLI does not account for radiation due to beam enrichment which can be an important fraction of the total radiation under some canopies (Canham *et al.* [7]).

To calculate precision of the GLI estimates, a random subset of the photos were selected and re-analyzed. The two major sources of imprecision were: 1) variation in the quality of the prints and 2) subjectivity in the selection of the appropriate threshold for digitizing photos. The maximum precision error in the data sets presented below was ±5% of the mean.

Study Sites and Sampling Design

The research areas on Whiteface Mountain, New York were located in an old-growth, montane forest on the northwest slope of the mountain (Table 1). One study grid (approximately 0.5 ha) was randomly located in the spruce-fir forest and one in the transition zone forest. Each rectangular grid was oriented with the long axis parallel to the contour and consisted of either a 5 x 10 (spruce-fir) or 6 x 8 (transition zone) arrangement of equally spaced points. The center of the grid in the spruce-fir was at 970 m in elevation; the transition zone plot was approximately 1 km downslope at 780 m elevation. In the spruce-fir forest, the dominant tree species are red spruce, (*Picea rubens* Sarg.), balsam fir (*Abies balsamea* (L.) Mill.) and mountain paper birch (*Betula papyrifera* Marsh. var *cordifolia* Regel). In the transition zone, red spruce along with three deciduous hardwood species — sugar maple (*Acer saccharum* Marsh.), American beech (*Fagus grandifolia* Ehrh.) and yellow birch (*Betula alleghaniensis* Britton) — are the most important tree species. A notable feature of the forest structure is the prevalence of standing dead spruce trees. Beginning in the mid-1960s, many adult red spruce in the forest died standing — the end result of a progressive loss of vigor (Battles and Fahey [2]). In 1990, fisheye photographs of the canopy were taken above each grid point.

Table 1. Ecological descriptions of the sites referred to in this study. Growing season was defined by either the frost-free interval (the three sites in the Northeastern United States) or the frost-free interval and soil moisture availability (the forest in the Sierra Nevada). K_T refers to the global atmospheric transmission coefficient. The superscript c indicates values calculated from site-specific solar radiation data; the superscript r refers to values taken from published regional averages.

	Whiteface Mountain[1]		Delaware Water Gap NRA[2]	Cornell Natural Areas[3]	Los Haitises National Park[4]	Blodgett Forest Research Station
Forest type	subalpine spruce-fir	conifer-hardwood transition zone	hemlock ravine	Allegheny northern hardwood	neotropical mangrove	Sierra Nevada mixed conifer
Leaf morphology	evergreen needle-leaved	deciduous broad-leaved; evergreen needle-leaved	evergreen needle-leaved	deciduous broad-leaved	evergreen broad-leaved	evergreen needle-leaved
Basal area (m^2/ha)	30.1	28.0	42.5	28.1 - 32.1	22.7	84.2
Tree density (stems/ha)	1766	1252	264	—	997	300
Canopy height (m)	mean: 8.1 max: 24.3	mean: 9.0 max: 26.4	mean: 27.5 max: 40.0	range: 21 - 24	mean: 24 max: 30	mean: 31.5 max: 49.9
Latitude	44° 22' N	44° 22' N	41° 31' N	42° 25' N	19°10' N	38° 52' N
Longitude	73° 54' W	73° 54' W	74° 49' W	76° 30' W	69° 40' W	120° 40' W
Growing season	Jun 1 - Sep 15	May 25 - Sep 15	Apr 15 -Sep 15	Apr 22 - Oct 15	Jan 1 - Dec 31	May 1 - Aug 31
K_T	0.47 ^{c}	0.47 ^{c}	0.46 ^{r}	0.50 ^{r}	0.49 ^{c}	0.70 ^{r}

[1] Data from Battles and Fahey [2] and Miller *et al.* [16]; [2] Data from Battles *et al.* [3]; [3] Data from Krasny and Whitmore [14]; [4] Data from Sherman *et al.* [23]

Resource managers at Delaware Water Gap National Recreation Area initiated intensive studies in two forested ravines dominated by eastern hemlock *(Tsuga canadensis* (L.) Carr.) and threatened by the exotic insect pest, the hemlock woolly adelgid (*Adelges tsugae* Annand.). Adams Creek and Van Campens Brook are tributaries to the Delaware River which forms the boundary of Pennsylvania and New Jersey (Table1). They are 5.5 km straight-line distance apart. Adams Creek is a third order stream which flows southeast off the Pocono Plateau. Elevation varies from 120 m at streamside to 280 m at the ravine edge. The ravine sides are steep and range from 12% to 80% slope. The study area consists of approximately 36 ha of hemlock-dominated forest along both sides of Adams Creek. The study area at Adams Creek was never cleared for agriculture; tree cutting was limited to small scale harvests for use on a private estate. Van Campens Brook is a second order stream and flows southwest into the Delaware River. Elevation ranges from 250 m at streamside to 350 m at the ravine edge. The ravine sides are gentler than those at Adams Creek and range from 3% to 25% slope. The study area encompasses about 18 ha with most of the hemlock-dominated woods on the north-northwest facing side of the stream. In contrast to Adams Creek, the Van Campens Brook study area was part of an agricultural community in the mid-1800's. To monitor the effect of adelgid feeding on the hemlock canopy, networks of permanent photo points were established in the two ravines. Random places along each stream were selected and points were located at the stream bank, 10 m, 30 m, and 50 m upslope from the stream edge. If an identifiable edge was within 100 m of the stream, a point was located on the edge of the hemlock canopy. A non-permanent point was also placed in the center of the stream to quantify canopy cover over the stream. There were 12 sets of photo points in Adams Creek and eight sets in Van Campens Brook. In 1994, hemispherical photographs of the canopy were taken above each point. The photos were taken before there was any measurable damage to the hemlock canopy from adelgid feeding.

The three sites that are part of Cornell University's Natural Areas are all located within a 10 km radius of Ithaca, New York (Table 1). These upslope sites represent relatively large contiguous tracts of old forest free from human disturbance for the last 65 years. Deciduous hardwood tree species comprise the forest canopy and include American beech, sugar maple, white ash (*Fraxinus americana* L.), red maple (*Acer rubrum* L.) and red oak (*Quercus rubra* L.). The North Mount Pleasant stand is approximately 8.7 ha in size; the Ringwood stand is 12.7 ha; and the Polson stand is 12.2 ha. All three stands are classified as the same vegetation association, namely the Allegheny northern hardwood forest. Krasny and Whitmore [14] established permanent sampling transects in these stands to monitor forest change. Agents of change in these stands include beech bark disease complex which causes dieback and mortality of infected American beech trees and periodic but non-fatal defoliation of canopy oak trees from gypsy moths (*Lymantria dispar* (L.). In 1994, canopy photos were taken at 12 random points along the transects in each stand (Newell [18]).

At Los Haitises National Park in the Dominican Republic, Sherman *et al.* [23] have studied the regeneration dynamics in a large tract (47 km^2) of undisturbed mangrove forest (Table 1). The forest is dominated by three, evergreen broad-leaved tree species: red mangrove (*Rhizophora mangle* L.), white mangrove (*Laguncularia racemosa* Gaertn), and black mangrove (*Avicennia germinans* L.). Twenty-three permanent vegetation plots were established along two transects that traversed the mangrove forest. In 1995, four canopy photographs were taken in each plot: one at a random location in each of the four quadrats. Three canopy photos were also taken near the center of 13 canopy gaps adjacent to the permanent plots. Most canopy gaps in this forest are caused by lightning strikes that typically kill all the trees in a 20-30 m diameter circular area. Based on measurements of 52 gaps, the average gap size was 506 m^2 (Sherman *et al.* [23]).

In 1997, I established a 1 ha plot in a mature mixed conifer forest at the Blodgett Forest Research Station in Georgetown, California (Table 1). The research plot was divided into a grid of 36 evenly spaced (20 m apart) points. All trees $\geq$19.5 cm diameter at breast height (dbh, 1.37 m) were tagged, identified, measured, and mapped. Fisheye photographs of the canopy were taken at each grid point. The research plot was located in the middle of compartment designated as a natural reserve. Aside from fire suppression, there has been no management activity since the stand was clear-cut around 1915. Constituent canopy tree species include white fir (Abies concolor Gordon and Glend.), Douglas-fir (*Pseudotsuga menziesii* (Mirbel) Franco var. *menziesii*), incense-cedar (*Calocedrus decurrens* (Torrey) Florin), ponderosa pine (*Pinus ponderosa* Laws.), sugar pine (*Pinus lambertiana* Douglas), and California black oak (*Quercus kelloggii* Newb.). A central subplot 0.36 ha in size (16 grid points) was used for detailed measurements of tree heights and crown shapes.

Analysis

Moran's I statistic was used to document spatial autocorrelation in GLI at the Whiteface Mountain sites (Legendre and Fortin [15]). Moran's I is a spatial analog to the familiar Pearson's correlation coefficient (R). It compares the covariance between pairs of points in a given distance class to the total variance in all the observations. Moran's I ranges from 1 to -1 with values greater than 0 indicating spatial autocorrelation (Legendre and Fortin [15]). The statistical significance of observed deviations was examined using randomization tests. Confidence intervals were generated by calculating Moran's I for 99 spatial randomizations of the GLI values. In each computer simulation, points in the grid were assigned a value at random and without replacement from the set of observed GLIs. In this way, any spatial covariance is removed without changing the overall variance in the data. The 96^{th} and 3^{rd} ranked values were taken as the upper and lower bounds of 95% confidence interval of the observed I (Crowley [9]). Standard parametric analyses were used to document differences in canopy parameters for within-site comparisons.

III. RESULTS

The forests in this study varied from closed canopy forests (e.g., Van Campens, Los Haitises-forest) with a gap fraction of 2% or less (Table 2) to more open forests affected by a diffuse disturbance (Whiteface Mountain, Battles and Fahey [2]). In all cases except for gaps in the mangrove forest and in the disturbed spruce-fir forest, canopy vegetation intercepted more than 80% of the available light (Table 2). Regardless of forest type, leaf morphology, or stand structure, gap fraction and GLI were closely correlated (R^2 = 0.94, $P < 0.04$, Table 2). Direct beam radiation contributed a greater percentage to the understory radiation regime in the tropical forest compared to the temperate forests in the humid and cloudy northeastern United States. However, only in the mixed conifer forest in the Sierra Nevada did direct beam radiation account for the majority of the transmitted understory light (Table 2).

There was significant positive autocorrelation in GLIs at a distance of 10 m for both reference grids at Whiteface Mountain (Figure 1). In the transition forest there were also indications of positive autocorrelation at 20 and 30 m distances. The autocorrelation in the transition forest was in part due to a significant linear decrease in GLI with distance away from a nearby stream: GLI = 26.3 - 0.29X where X = distance from stream (R^2 = 0.37, $P < 0.01$, Figure 1). In contrast, there was no spatial trend in the gap fraction with distance from the stream for the two hemlock ravines in the Delaware Water Gap National Recreation Area (General Linear Model, P = 0.68, Figure 2). Interestingly, one of the darkest places in the hemlock ravine

Table 2. Summary of canopy metrics calculated from fisheye photographs at the five research sites. The mean and standard deviation (s.d.) is given for each metric; n refers to the total number of samples. % beam radiation is the estimated percentage of transmitted light that is direct beam radiation. For within-site comparisons, metrics followed by different superscripts are significantly different at a level of $P < 0.05$.

	Whiteface Mountain		Delaware Water Gap NRA (ravine only)		Cornell Natural Areas			Los Haitises National Park[1]		Blodgett Forest
	spruce-fir	transition	Adams Creek	Van Campens	Polson	Ringwood	N. Mount Pleasant	Gap	Forest	mixed conifer
Gap fraction										
mean	14.9 [a]	14.5 [a]	4.3[a]	2.2[b]	6.5 [a]	4.1[b]	4.1 [b]	10.8 [a]	1.6 [b]	7.4
s.d.	7.3	6.5	2.1	1	2.1	3.2	2.1	5.2	1.5	2.1
Gap light index (GLI)										
mean	21.7 [a]	19.1 [a]	6.3 [a]	3.4 [b]	8.2 [a]	5.0 [b]	5.2 [b]	23.2 [b]	2.8 [b]	11.6
s.d.	10.4	8.1	3.2	1.9	2.2	2.4	2.8	10.6	1.4	4.6
% Beam Radiation										
mean	34 [a]	35 [a]	36 [a]	32 [a]	31 [a]	37 [a]	33 [a]	46 [a]	41[b]	67
s.d.	6	7.3	8.3	14	14	11	10	3	5.7	10
n	50	48	36	24	12	12	12	13	23	36

[1] The difference in GLI between gaps and forest plots for the mangrove forest in Los Haitises National Park was previously published in Sherman *et al.* [23].

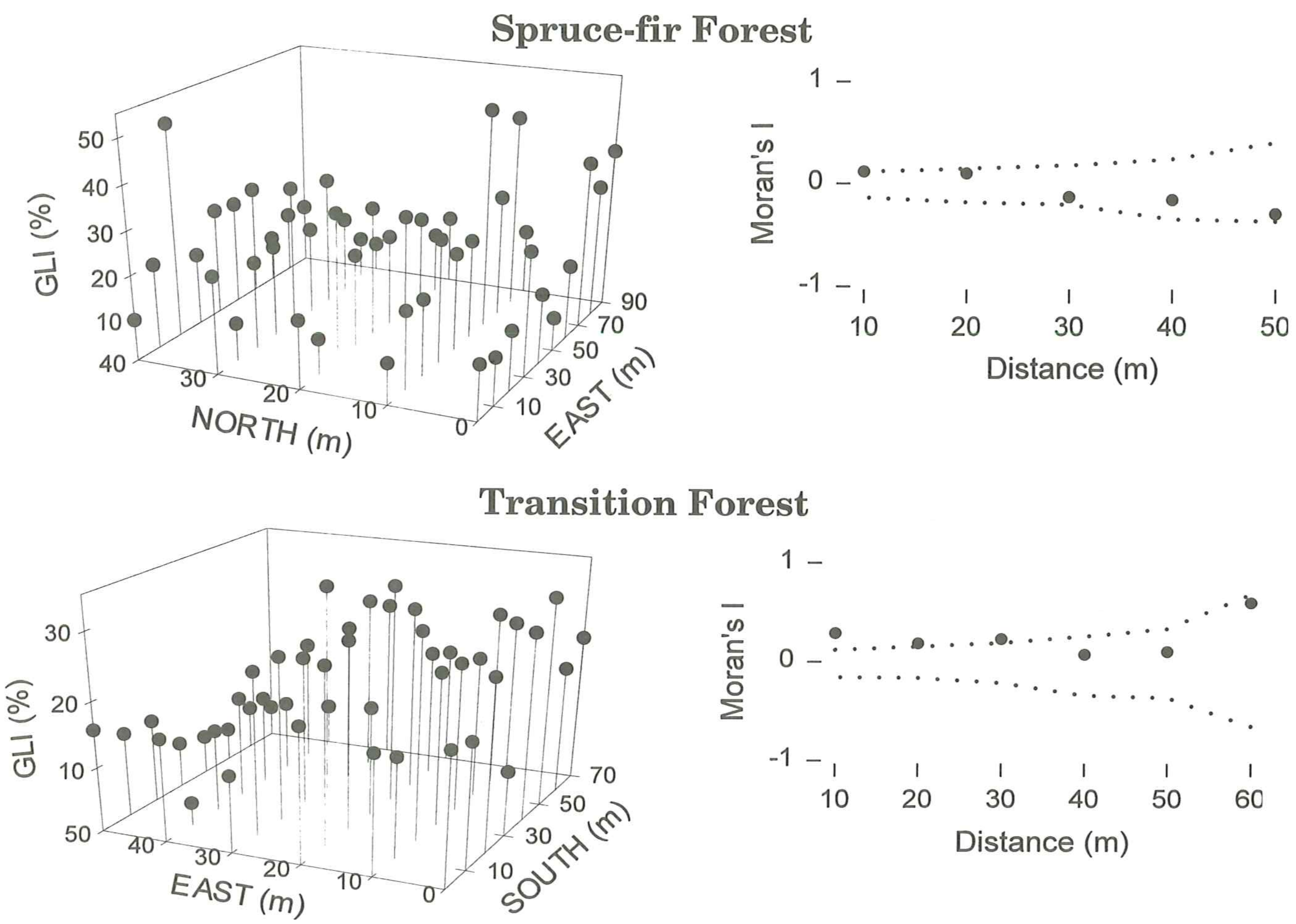

Figure 1. Spatial patterning in the understory light regime in the reference grids at Whiteface Mountain. GLI is the estimated gap light index at 1.2 m above ground. The 3D plots on the left show the GLI on the Z-axis and location on X-Y plane. The corresponding plot of spatial autocorrelation (Moran's I) is to the right of the 3D plots. The dotted lines indicated 95% confidence intervals for each distance. The solid circles are the observed value of Moran's I at each distance. N = 50 in the spruce-fir forest; N = 48 in the transition forest.

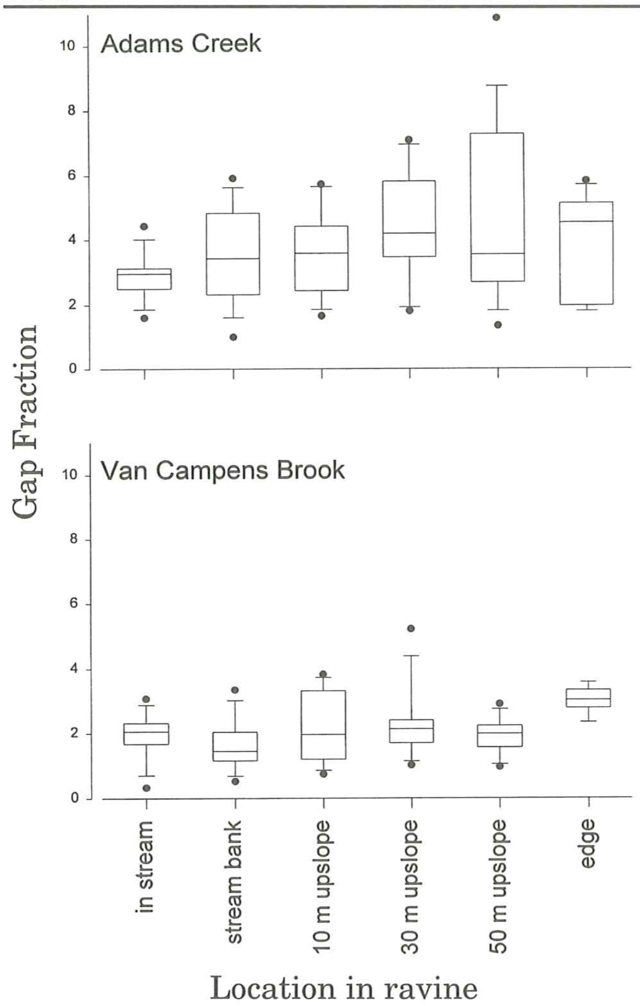

Figure 2. Box plots of the gap fraction derived from canopy photographs at different locations in the two hemlock ravines at Delaware Water Gap National Recreation Area. The top and bottom of the box are drawn at the upper and lower quartiles; the box is divided at the median. The lower and upper whiskers represent the 10th and 90th quantiles. Outliers are plotted as circles.

was in the middle of the stream (Figure 2).

Within a particular forest type, there was significant variation in gap fraction and GLI among stands. Gap fraction and GLI were significantly greater in the hemlock forest at Adams Creek compared to Van Campens Brook (Table 2) and the difference was consistent across the various locations in the ravine (Figure 2). Among the three stands in the Cornell Natural Areas, the canopy was more open and more light reached the understory at the Polson tract than at the other two stands (Table 2).

The canopy architecture in the mangrove forest at Los Haitises National Park was strongly bimodal in terms of the frequency distribution of gap fraction and GLI. As noted by Sherman *et al.* [23], very little light reaches the understory of this mangrove forest (Table 2) outside of lightning gaps. Under gaps, the light regime is significantly enriched.

In the mixed conifer stand at Blodgett Forest, the frequency distribution of GLIs followed a more unimodal distribution. Aside from one very dark spot in the understory, most microsites received between 6 and 18% of incident radiation (Figure 3). Clearly the vertical and horizontal spatial structure of canopy trees influenced the understory light environment. Points receiving greater than average light corresponded to places where adult trees have recently died (Figure 3).

IV. DISCUSSION

Fine-scale autocorrelation of light penetrating forest canopies is an expected result given the constraints on tree crown shapes, the predictability of solar geometry, and the principles of penumbral optics (Horn [11], Reifsnyder *et al.* [19], Smith *et al.* [25]). In two neotropical rainforests, indices of understory light were correlated at distances from 2.5 m to 12.5 m (Becker and Smith [4], Smith *et al.* [24], Clark *et al.* [8]). In a mature pine plantation, Walter and Gregoire Himmler [28] reported spatial autocorrelation up to 10 m. We detected spatial autocorrelation in light availability at a similar scale in the subalpine forest at Whiteface Mountain (Figure 1). Only recently have autocorrelation analyses been used to investigate the spatial structure of canopy variables. Such results can guide decisions about the necessary minimum resolution in remote sensing applications. For example in the spruce-fir forest, pixel sizes greater than 10 m may be adequate to reliably estimate some canopy parameters.

In addition to the expected fine-scale autocorrelation of light values, there can also be significant coarser-scale trends. I was surprised by the extent of the influence of a stream channel on understory light availability in the transition forest at Whiteface Mountain (Figure 1). The stream is a small, first order drainage with a channel < 4 m in width. The edge of the grid closest to the stream was at least two adult tree crowns away from the bank (approximately 15 m). Yet the effect of the stream opening was still measurable 45 m from the water. This result highlights the influence that even small geomorphological features can have on canopy architecture and the understory light regime.

The lack of any detectable correspondence between distance-from-stream and gap fraction in the hem-

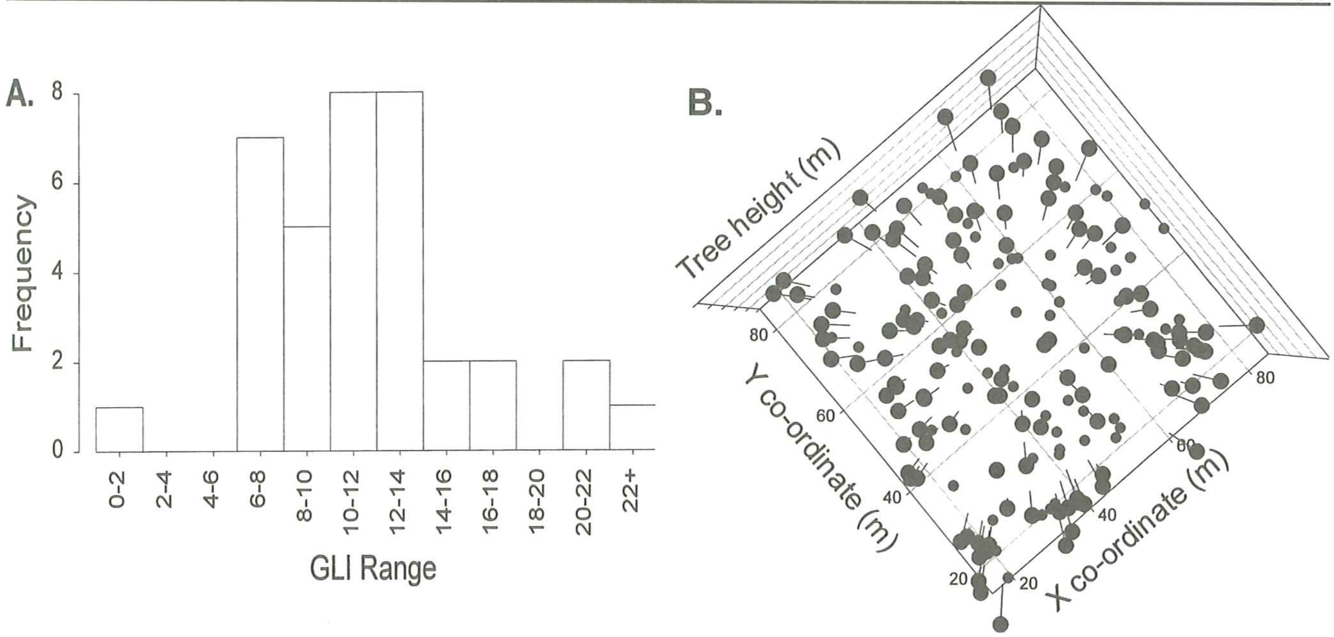

Figure 3. A. The frequency distribution of GLI values for the 36 grid points in the mature mixed conifer forest at the Blodgett Research Station. B. 3D-view looking down on the canopy showing the vertical and horizontal structure. Large circles are live trees; smaller circles are standing dead trees.

lock ravines at Delaware Water Gap presents an interesting alternative result to what was observed in the transition zone forest (Figure 2). Canham *et al.* [7] reported that tree crown geometry has an important effect on the spatial variation in understory light regimes. Hemlock trees, in particular, were noted for the distinctively deep shade cast by their crowns, an effect attributed to the depth of their crowns. Hemlock trees cast a great deal of shade because their foliage extends low enough to block incident radiation at angles 20-40°from the vertical (Canham *et al.* [7]). This crown geometry may have masked differences introduced by topography and contributed to the remarkably consistency of the canopy architecture found throughout the ravine. Such quantification of the structural variability of the canopy is precisely the kind of information needed to measure estimation error in satellite based monitoring of hemlock forest health (Royle and Lathrop [22]).

In ecosystem modeling and remote sensing research, landscapes are often divided into vegetation classes or plant functional types in order to predict or measure variables of interest (e.g., productivity, leaf area index, radiative transfer, see Woodward and Cramer [29]). While responses are expected to vary for different landscape units categorized as the same type, this within-type variability is rarely assessed but perhaps should be. For example, the two hemlock ravines at Delaware Water Gap and the three northern hardwood stands in Cornell Natural Areas had significant differences in gap fraction and GLI (Table 2). These stands were specifically selected to be replicates. They are similar with regard to forest age, land-use history, and species composition. The difference between the hemlock ravines is again likely related to hemlock crown geometry. At Van Campens Brook, trees are shorter and crown depth is greater (Battles *et al.* [3]). Thus more light is intercepted by the canopy trees (Table 2). For the Cornell Natural Areas, the significantly more open canopy in the Polson tract (Table 2) may be due to small differences in forest composition. The shade tolerant American beech is more abundant at Ringwood and Mount Pleasant stands than at the Polson stand (Krasny and Whitmore [14]). Like hemlock, beech trees tend to cast deep shade (Canham *et al.* [7]). Whatever the cause, the heterogeneity within a vegetation class needs to be measured before assuming it can be ignored.

Viewed from above, the surface of the mangrove forest canopy at Los Haitises National Park looks like a smooth green surface with distinct holes punched in it. Because of the sharp break between forest and gap, the canopy structure can accurately be classified as either intact or open. This clear distinction between gap and intact forest is not typical. Gaps in the forests at Whiteface Mountain and the Cornell Natural Areas are difficult to distinguish from the background. The inherent variability of these temperate forests coupled with disturbances that leave standing dead trees which continue to intercept light produce a broad gradient in understory light availability (Battles and Fahey [2], Newell [18], Krasny and Whitmore [14]).

Despite the bimodal nature of the canopy structure in the mangrove forest, parameters of the mangrove canopy can be reliably determined from very coarse-scale remote sensing data. Lightning gaps account for less than 2% of the land area in the mangrove (Sherman *et al.* [23]). Given the uniformity of the remaining 98% of the canopy, it is likely that only small errors will be introduced if gaps are neglected.

The work in the mixed conifer forest at the Blodgett Research Station is part of an effort to quantify the light climate of tree saplings growing in the understory. This data collected to answer ecological questions about plant performance also is ideal for validating photo ecometric techniques for measuring properties of individual trees. All of the photo grid points and trees are mapped to UTM coordinates. Not only is the position known for every canopy tree but also its height, crown depth, crown width, and crown shape.

In a recent paper, Blackburn and Milton [5] provide an example of how remote sensing can serve the needs of woodland ecology. This paper describes what woodland ecology can offer to remote sensing. Fisheye photography is becoming a widely-used technique in forest ecology. Two commercial versions of the equipment and software are available; a third is in production. Advances in digital photography will further ease the use of this technology. While validation and ground truthing will remain essential services that ecology provides to remote sensing, the emergence of photo ecometric techniques such as fisheye photography have the potential to render spatially explicit information at scales relevant to applications in remote sensing.

ACKNOWLEDGMENTS

Funding for this research was provided by the California Agricultural Experiment Station, the Kieckhefer Foundation, the US National Park Service, the A.W. Mellon Foundation and the National Science Foundation. M. Krasny kindly provided access to her data from the Cornell Natural Areas.

REFERENCES

[1] Adams, J.M. Towards a better vegetation scheme for global mapping and monitoring. Global Ecology and Biogeography Letters 5: 3-6.

[2] Battles, J. J., and T. J. Fahey. In revision. Recovery from forest decline: A case study of red spruce forests, northeastern USA. Ecological Applications.

[3] Battles, J.J., N. Cleavitt and T.J. Fahey. 1997. Final Report — Quantitative assessment of the understory vegetation of two eastern hemlock stands in the Delaware Water Gap National Recreation Area. National Park Service, Research and Resource Planning, Milford, Pennsylvania.

[4] Becker, P., and A. P. Smith. 1990. Spatial autocorrelation of solar radiation in a tropical moist forest understory. Agricultural and Forest Meteorology 52:373-379.

[5] Blackburn, G A., and E.J. Milton. 1996. Filling the gaps: Remote sensing meets woodland ecology. Global Ecology and Biogeography Letters 5:175-191.

[6] Canham, C.D. 1988. An index for understory light levels in and around canopy gaps. Ecology 69:1634-1637.

[7] Canham, C.D., A.C. Finzi, S.W. Pacala, and D.H. Burbank. 1994. Causes and consequences of resource heterogeneity in forests: Interspecific variation in light transmission by canopy trees. Canadian Journal of Forest Research, 24:337-349.

[8] Clark, D. B., D. A. Clark, P. M. Rich, S. Weiss, and S. F. Oberbauer. 1996. Landscape-scale evaluation of understory light and canopy structure: methods and application in a neotropical lowland rainforest. Canadian Journal of Forest Research 26:747-757.

[9] Crowley, P. H. 1992. Resampling methods for computation-intensive data analysis in ecology and evolution. Annual Review of Ecology and Systematics 23:405-447.

[10] Gong, P., G.S. Biging, S.M. Lee, X. Mei, Y. Sheng, R. Pu, B. Xu, K. Schwarz and M. Mostafa. Photo ecometrics for forest inventory. Geographic Information Sciences 5(1):9-14.

[11] Horn, H.S. 1971. The adaptive geometry of trees. Princeton University Press, Princeton, New Jersey, USA.

[12] Howard, D.C., R.M. Fuller, and C.J. Barr. 1996. Linking ecological information recorded from ground, air, and space: examples from Countryside Survey 1990. Global Ecology and Biogeography Letters 5: 227-234.

[13] Knapp, C. L., T. L. Stoffel, and S.D. Whitaker. 1980. Insolation data manual: long term monthly averages of solar radiation, temperature, degree-days, and global K_T for 248 National Weather Service stations. Solar Energy Research Institute, Washington, D.C., USA.

[14] Krasny, M. E., and M. C. Whitmore. 1992. Gradual and sudden forest canopy gaps in Allegheny northern hardwood forests. Canadian Journal of Forest Research 22:139-143.

[15] Legendre, P., and M. Fortin. 1989. Spatial pattern and ecological analysis. Vegetatio 80:107-138.

[16] Miller, E. K., A. J. Friedland, E. A. Arons, V. A. Mohnen, J. J. Battles, J. A. Panek, J. Kadlecek, and A. H. Johnson. 1993. Atmospheric deposition to forests along an elevational gradient at Whiteface Mountain, NY USA. Atmospheric Environment A 27:2121-2136.

[17] Nemani, R. and S. Running. 1997. Land cover characterization using multitemporal red, near-IR, and thermal-IR data from NOAA-AVHRR. Ecological Applications 7: 79-90.

[18] Newell, M. 1995. Gap light distribution in northern hardwood forests. Undergraduate thesis. Cornell University, Ithaca, New York.

[19] Reifsnyder, W. E., G. M. Furnival, and J. L. Horowitz. 1971. Spatial and temporal distribution of solar radiation beneath forest canopies. Agricultural Meteorology 9:21-37.

[20] Rich, P.M. 1989. A manual for analysis of hemispherical canopy photography. Los Alamos National Laboratory Report LA-11733-M.

[21] Rich, P.M. 1990. Characterizing plant canopies with hemispherical photographs. *In* N.S. Goel and J.M. Norman, editors. Instrumentation for studying vegetation canopies for remote sensing in optical and thermal infrared regions. Remote Sensing Reviews 5:13-29.

[22] Royle, D.D. and R.G. Lathrop. 1997. Monitoring hemlock forest health in New Jersey using Landsat TM data and change detection techniques. Forest Science 43: 327-335.

[23] Sherman, R.E., T.J. Fahey, and J.J. Battles. In revision. Small-scale disturbance and regeneration dynamics in a neotropical mangrove forest. Journal of Ecology.

[24] Smith, A.P., K.P. Hogan, and J.R. Idol. 1992. Spatial and temporal patterns of light and canopy structure in a lowland tropical moist forest. Biotropica 24:503-511.

[25] Smith, W. K., A. K. Knapp, and W. A. Reiners. 1989. Penumbral effects on sunlight penetration in plant communities. Ecology 70:1603-1609.

[26] Spitters, C. J. T., H.A.J.M. Toussaint and J. Goudriaan. 1986. Separating the diffuse and direct component of global radiation and its implications for modeling canopy photosynthesis: Part I. Components of incoming radiation. Agricultural and Forest Meteorology 38:217-230.

[27] Stoffel, T. L. 1980. Global K_T methodology. Pages 252-253 *in* C. L. Knapp, T. L. Stoffel, and S.D. Whitaker. Insolation data manual: long term monthly averages of solar radiation, temperature, degree-days, and global K_T for 248 National Weather Service stations. Solar Energy Research Institute, Washington, D.C., USA.

[28] Walter, J. M. N. and C. Gregoire Himmler.1996. Spatial heterogeneity of a Scots pine canopy: An assessment by hemispherical photographs. Canadian Journal of Forest Research 26:1610-1619.

[29] Woodward, F.I. and W. Cramer, editors. 1996. Special feature: Plant functional types and climatic changes. Journal of Vegetation Science 7: 306-425.